Potential-induced breathing model for the elastic moduli and high-pressure behavior of the cubic alkaline-earth oxides

M. J. Mehl*
Naval Research Laboratory, Washington, D.C. 20375-5000

R. J. Hemley
Geophysical Laboratory, Carnegie Institution of Washington, Washington, D.C. 20008

L. L. Boyer
Naval Research Laboratory, Washington, D.C. 20375-5000
(Received 10 January 1986)

A parameter-free model is presented for the elastic constants and high-pressure behavior of the alkaline-earth oxides MgO, CaO, SrO, and BaO. The model is based on a Gordon-Kim-type calculation for the short-range energy of a crystal. Spherically symmetric relaxation of ion charge density in response to the Madelung potential, termed potential-induced breathing (PIB), is incorporated into the model as a function of strain. This charge relaxation is accomplished by the use of a Watson-sphere calculation to obtain the interaction energy of pairs of ions as a function of both interatomic distance and Coulomb potential. By this technique many-body effects, which are particularly important for the prediction of crystal elasticity, are included. The model successfully reproduces both the sign and magnitude of the deviation ($\Delta = C_{12} - C_{44}$) from the Cauchy relation measured at zero pressure for the cubic alkaline-earth oxides. Static compression curves calculated in both the $B1$ and $B2$ phases of these compounds are found to be within 5% of the available room-temperature data. From a calculation of the pressure dependence of the elastic moduli, the role of many-body effects at high pressure is determined. The $B1$-$B2$ phase transition pressures are calculated within the PIB model to be 251 GPa (MgO), 55 GPa (CaO), 36 GPa (SrO), and 21 GPa (BaO), in very good agreement with available experimental data for these compounds.

I. INTRODUCTION

The elastic moduli of crystalline solids have often been used to characterize their static and dynamical properties.[1] As prototype ionic crystals, the alkali halides have received considerable attention in this regard. A number of calculations of their elastic moduli have been performed based largely on the ionic model.[2] For the alkaline-earth oxides, which have the $B1$ (NaCl-type) structure, the question of ionicity and the proper characterization of the charge density has required more extensive studies.[2-8] The earliest attempts to calculate properties of the alkaline-earth oxides from first principles, i.e., without adjustable parameters, were based on the assumption of two-body, central forces between rigid ions.[3,4] Extensions of these calculations[5,7] to include many-body contributions were found to give good predictions of the binding energies, lattice parameters, and equations of state of these solids.

For the calculation of the elastic moduli, models based on two-body central forces necessarily fail to reproduce the measured deviation from the Cauchy equality ($C_{12} = C_{44}$ for cubic crystals). This equality must hold for an unstressed lattice at its minimum energy configuration ($P = 0$) if the lattice energy is determined by strictly pairwise interactions between the component ions. Vibrational pressure produces a violation of the Cauchy relation, but this is generally small compared to that observed experimentally. Thus, the degree of departure from the Cauchy condition is a measure of the noncentral or many-body terms in the crystal potential.[2] The deviation from the Cauchy condition ($\Delta = C_{12} - C_{44}$) is particularly large and negative for MgO, and decreases through the series of alkaline-earth oxides, becoming positive for BaO.[9-13] Semi-empirical models achieve a Cauchy violation by removing the constraint of rigid ions to give an effective many-body interaction, or by directly including many body terms in some parametrized form, or both. These models have not been implemented at the first-principles (parameter-free) level, however, nor have they included, even in parametrized form, the particular nonrigid-ion effect which we obtain from first-principles calculations.

The presure dependence of the elastic moduli can provide useful information of the nature of the many-body forces producing the Cauchy violation. The extent to which the Cauchy violation affects the pressure dependence of the elastic moduli has not yet been examined from first principles. On intuitive grounds it may be expected that the many-body forces increase with compression. Therefore, as a starting point for calculations it would appear that the measured Cauchy violation at $P = 0$ be satisfied before reliable predictions can be made for the behavior at high pressure. For the cubic alkaline-earth oxides experimental static compression data have been obtained.[14-20] From these data estimates of the bulk moduli and their pressures derivatives have been determined. Although information on the individual C_{ij} is

more limited, a number of studies of the pressure dependence of individual elastic moduli have been undertaken experimentally.[9-13] The C_{ij} for MgO have been measured[13] to a pressure of ~ 3 GPa.

Several alkaline-earth oxides exhibit polymorphism at high pressure. CaO and SrO have been shown to transform to the $B2$ (CsCl) structure at ~ 65 GPa (Refs. 16, 17, and 21) and ~ 36 GPa (Ref. 19) respectively; BaO appears to transform to a distorted $B2$ phase at ~ 10 GPa (Ref. 20). Theoretical predictions for the pressure of the $B1$-$B2$ transition in MgO range from 110 to 1050 GPs.[3,22-25] Information on the elastic properties of those high-pressure phases that have been observed experimentally is difficult to obtain. Although empirical equations of state have been fit to the existing pressure-volume data for the high-pressure phases, such analyses are often poorly constrained by the data as a result of the strong dependence of the equation of state on the often hypothetical zero-pressure bulk modulus of the high-pressure phase (see Ref. 19). This problem is particularly important for determining the pressure dependence of elasticity, equations of state, and phase transitions in materials that may be of geophysical importance such as the close-packed (i.e., sixfold and eightfold coordinated) oxide phases studied here.[26,27]

Recently, first-principles calculations have been carried out based on a model for ionic solids that incorporates the effect of spherically symmetric charge relaxation in response to the Madelung potential at the site of the ions.[8] In other words, the ion charge density is allowed to contract and expand as the electrostatic potential at the site of the ion is raised and lowered, respectively. This potential-induced breathing (PIB) model was shown to give a good account of the Cauchy violation in MgO as well as contribute substantially to the splitting of the longitudinal optic (LO) and transverse optic (TO) modes in the alkaline-earth oxide and alkali-halide crystals. The model utilizes charge densities of the component ions calculated from relativistic atomic self-consistent-field (SCF) calculations[28] employed with a generalized Watson-sphere model.[29]

From the charge densities pair potentials are obtained by the use of density-functional techniques.[30-33] The pair potentials are functions of both the interionic distance and the Watson-sphere (shell) potential, the latter dependence providing the effective many-body contribution.

Although superficially similar to the breathing-shell model,[34] the PIB approach is fundamentally different by virtue of the fact that the relaxation of charge density is coupled directly to the Madelung potential; in the breathing-shell model the breathing is accomplished by short-range interaction with near neighbors. An inherent limitation of the breathing-shell model is its inability to obtain a positive Cauchy violation at equilibrium[2] (i.e., C_{44} is always greater than C_{12}). The distinction between the two approaches is brought out in the present paper by the fact that the PIB model is able to reproduce correctly both positive and negative Cauchy violation found experimentally for the class of materials studied here.

The present paper is concerned with the second-order elastic moduli and high-pressure behavior of the alkaline-earth oxides in the $B1$ (NaCl) and $B2$ (CsCl) phases. A similar model has been used recently to calculate the equation of state of MgO ($B1$ phase).[7] In that study the ionic charge densities were determined by the Hartree-Fock HF-SCF method and the pair potentials calculated by modified electron gas (MEG) techniques. Comparison between the present results and those obtained from the HF-SCF technique will be examined in detail in a subsequent paper. All calculations reported here are for the static lattice (no zero point or thermal contributions). The effect of potential-induced breathing on the quasiharmonic lattice dynamics and thermal properties will be presented elsewhere.

In Sec. II the theoretical methods are outlined, including the procedure used to fit the numerical potentials to an accurate and effective analytic form. The elastic moduli at zero pressure are presented and discussed in Sec. III. The compression curves (equations of state) calculated for the static lattice from the PIB model are presented in Sec. IV. The calculated pressure dependence of the elastic moduli in the $B1$ and $B2$ phases, including a discussion of low- and high-pressure instabilities, are given in Sec. V. In Sec. VI, PIB theory predictions for the $B1$-$B2$ transitions in the alkaline-earth oxides are presented. The possibility of other phase transitions for MgO is also considered. Section VII contains a discussion and concluding remarks.

II. THEORY AND PARAMETRIZATION

In the original applications of the Gordon-Kim model to ionic crystals, the total charge density was assumed to consist of overlapping rigid-ion charge densities. In fact, the first calculations used free-ion charge densities, although this is not necessary.[3-6] When the real crystal is constructed from free ions, a relaxation of charge density occurs in response to the crystal potential.[4,5] Moreover, when a crystal lattice is strained, the electron density relaxes in response to changes in the crystal potential. The lowest-order description of this response is the spherically symmetric relaxation of charge density, termed "potential induced breathing". The rigid-ion model is particularly suspect in the oxides, because free O^{-2} is not stable; therefore, the oxygen part of the electron density, stabilized by the crystal potential, will be highly susceptible to changes in the lattice. What is required is a simple means of coupling the electrons around each ion to the changes in the crystal lattice.

In this paper we couple the electrons to the lattice by use of the PIB model.[8] The crystal is assumed to consist of overlapping ions. The electron density of each ion is found by a self-consistent relativistic calculation,[28] using the local-density approximation with an average self-interaction correction,[32] and the Hedin-Lundqvist[33] parametrization for the correlation energy. The crystal potential is approximated by use of a Watson sphere.[29] Specifically, we center the nucleus of the ion inside a uniformly charged spherical shell, with a total charge chosen to neutralize the ion (thus the sphere around a O^{-2} ion would have charge $+2e$). The radius of the sphere is chosen so that the electrostatic potential inside the shell is

identical to the long-range (Madelung) potential at the site of the nucleus when the ion is in the lattice (see Refs. 4 and 5). The pairwise interactions between ions, which depend on the ionic charge densities in the original Gordon-Kim model, are now dependent on the crystal structure. In addition, the self energy of the ion (that is, the energy required to assemble the electrons around the nucleus) is now a function of the site potential.

Within the pairwise interaction approximation, the total energy of the crystal may be written in the form

$$\Phi=\tfrac{1}{2}\sum_{k,l} Z_k P(l_k)+\sum_{l,k} S_k(P(l_k)) + \tfrac{1}{2}\sum_{k,k',l,l'}{}' \phi_{kk'}(P(l_k),P(l'_{k'}),|\mathbf{r}(l_k)-\mathbf{r}(l'_{k'})|)\ , \quad (1)$$

where $P(l_k)$ is the Madelung potential at the site (l_k),

$$P(l_k)=\sum_{k',l'}{}' \frac{Z_{k'}}{|\mathbf{r}(l_k)-\mathbf{r}(l'_{k'})|}\ , \quad (2)$$

Z_k is the net charge on the kth ion, S_k is the self-energy of the kth ion [which is coupled to the lattice through $P(l_k)$], and $\phi_{kk'}$ is the "short-range part" of the interaction between the kth and k'th ions. The prime on the summation signs indicates that the $(l_k)=(l'_{k'})$ terms are omitted. Within the Gordon-Kim approximation,

$$\phi_{kk'}(P_k,P_{k'};\mathbf{R})=E[n_k(P_k,\mathbf{r})+n_{k'}(P_{k'},\mathbf{r}-\mathbf{R})] -E[n_k(P_k,\mathbf{r})]-E[n_{k'}(P_{k'},\mathbf{r}-\mathbf{R})]\ , \quad (3)$$

where $n_k(P,\mathbf{r})$ is the charge density of an ion of type k in a Watson sphere with interior potential P, and $E[n]$ is a sum of functionals obtained in the local-density approximation (LDA). In atomic units ($\hbar=e=m=1$; distances in Bohrs and energies in Hartrees),

$$E[n(\mathbf{r})]=\tfrac{3}{10}(3\pi^2)^{2/3}\int d^3r[n(\mathbf{r})]^{5/3}+\tfrac{1}{2}\int d^3r\int d^3r'\frac{n(\mathbf{r})n(\mathbf{r}')}{|\mathbf{r}-\mathbf{r}'|} -\tfrac{3}{4}(3/\pi)^{1/3}\int d^3r[n(\mathbf{r}')]^{4/3}+\int d^3r\, n(\mathbf{r})\epsilon_c[n(\mathbf{r})]+\int d^3r\, v_{\rm ext}(\mathbf{r})n(\mathbf{r})\ . \quad (4)$$

The first term is the Thomas-Fermi kinetic energy. The second and third terms are the (exact) Coulomb and local exchange energies, respectively. In this paper the Hedin-Lundqvist parametrization of the LDA correlation energy ϵ_c is used.[33] In the last term, $v_{\rm ext}(\mathbf{r})$ is the Coulomb potential of the two nuclei. The ionic self-energies S_k are also calculated by the use of the functional (4), with $v_{\rm ext}(\mathbf{r})=-Z_k/|\mathbf{r}|$, and with self-interaction corrections[32] to the exchange and correlation energies included. The Madelung contribution to the total energy can be calculated by use of the Ewald technique.[35]

To speed the calculations, numerical values of the self-energies S_k and the short-range pair interaction $\phi_{kk'}$ are fit to analytic functions for interpolation between computed values. First, the range of Madelung potentials needed is determined for each ion. Then, the charge density for each ion is calculated self-consistently for several (on the order of 10) potentials in this range. The self-energy of each ion is fit to a quartic polynomial in the Madelung potential. The resulting polynomial is accurate to about 10^{-5} hartree for the range of potentials used in this paper.

The short-range pair interactions [Eq. (3)] are divided into six parts, as described in the Appendix, and each part is parametrized. Typically, the largest error in the parametrized potential is 2–5%, and it is usually this large only at rather small distances (the largest errors are at $R=2$ bohr in the Mg-O potential). To check the accuracy of the parametrization, the energy of MgO in the rocksalt phase was calculated as a function of the lattice constant in two ways. First the parametrized self-energies and potentials were used, and second, the charge densities, self-energies, and pair interaction potentials at each volume were calculated explicitly. Only the nearest-neighbor Mg-O and O-O interactions were used for this test. The results of both calculations are plotted in Fig. 1. There is no apparent error in the parametrized form except at very small volumes. Since, as we shall see, the PIB model is accurate to at most several percent, the parametrization scheme is more than adequate for our needs.

The parametrized form of the potentials substantially simplifies the calculations, because the total energy [Eq. (1)] can be expressed analytically as a function of the lattice strain. First derivatives are evaluated analytically within this model. Second derivatives are calculated by the use of the exact first derivatives and the five-point Lagrange numerical interpolation formula.[36]

The final computational approximation is the trunca-

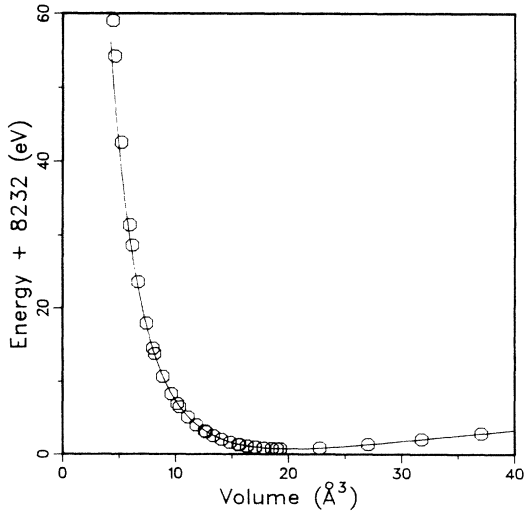

FIG. 1. Calculated total energy versus volume for MgO in the PIB model, showing the difference between the numerical calculations (circles) and the parametrized form as discussed in the Appendix (solid line). The parametrized form is accurate for unit-cell volumes between 8 and 40 Å^3.

TABLE I. Equilibrium lattice constants of the cubic alkaline-earth oxides.

MgO		CaO		SrO		BaO	
Calc.[a]	Expt.[b]	Calc.[a]	Expt.[b]	Calc.[a]	Expt.[b]	Calc.[a]	Expt.[b]
4.30	4.211	4.82	4.810	5.13	5.16	5.49	5.54
4.58[c]		4.94[c]					
4.34[d]							
4.260[e]							
4.293[f]							

[a]The first line gives the PIB result. Static lattice calculations, except where noted.
[b]Room-temperature data (see Ref. 36).
[c]MEG, Cohen and Gordon (Ref. 3). Watson-sphere [(4)—(5)] model.
[d]SSMEG, Muhlhausen and Gordon (Ref. 4).
[e]Boyer (Ref. 6). Room-temperature.
[f]SSMEG, Hemley *et al.* (Ref. 7).

tion of the sum over ion pairs in the short-range part of the potential. After the third nearest neighbors of all types (i.e., third nearest Mg-Mg, O-O, and Mg-O pairs in MgO) the short-range sum in the total energy is essentially converged: on a graph similar to Fig. 1 there is no apparent difference between the curves calculated by truncating at the third- or fourth-neighbor shell, except at small volumes beyond our interest. This result is valid for all the compounds and lattices discussed in this paper.

III. EQUILIBRIUM CALCULATIONS

This section is devoted to the equilibrium properties of the experimentally stable low-pressure $B1$ (rocksalt) phases of the alkaline-earth oxides MO, where M=Mg, Ca, Sr, or Ba. Questions of the stability of this phase within PIB and under pressure will be considered in Sec. VI. The calculated equilibrium lattice constants are compared with the experimental results[37] in Table I. The results of other Gordon-Kim—type calculations.[4,6,7] are also listed for MgO and CaO. Because the present theory does not as yet include zero-point motion or temperature effects,[6,7] both of which would tend to increase the lattice constant, it is seen that the present treatment generally overestimates the equilibrium lattice constants for these crystals.

The cohesive energies of MgO and CaO are calculated following the method of Cohen and Gordon.[3] The free-ion total energies were calculated by setting the Watson-sphere potential to zero for each ion. Table II gives the energy required to drive the reaction

$$MO(\text{solid}) \rightarrow M^{2+}(\text{free ion}) + O^{-}(\text{free ion}) + e^{-}$$

for M=Mg and Ca. The fourth column lists the experimental cohesive energies, as tabulated in Ref. 3. The second column lists the cohesive energy using the PIB energy [Eq. (1)], with the kinetic part of the ion self-energies calculated in the Thomas-Fermi approximation [the $n^{5/3}$ term in Eq. (4)]. This approximation gives cohesive energies that are about 30% smaller than found by experiment. In the third column the cohesive energies calculated by the method of Kohn and Sham[38] are shown; the use of this method is discussed in detail in Sec. VIII, where possible improvements in the model are outlined.

TABLE II. Cohesive energies (eV per molecule).

	MEG[a]	PIB		Expt.[a]
		Thomas-Fermi	Kohn-Sham	
MgO	30.7	21.4	33.5	31.5
CaO	28.0	19.1	30.1	37.4

[a]See Cohen and Gordon (Ref. 3).

The PIB elastic moduli at equilibrium are compared to the room-temperature experimental and the rigid-ion modified electron gas results[3] in Table III. The PIB moduli were found by numerically differentiating the exact first derivatives, as outlined in Sec. II. The bulk modulus was calculated from the second derivative of the energy with respect to volume. The C_s modulus was found by stretching (contracting) the lattice in the [001] direction, with a volume preserving contraction (stretch) in the plane perpendicular to [001]. C_{44} was determined by stretching (contracting) the lattice in the [111] direction, and then contracting (stretching) uniformly in the [111] plane to preserve the volume.

There are several points of interest in Table III. The most important is that the Cauchy equality demanded of rigid-ion pair potential models has been broken. Although many-body interactions are not explicitly considered in calculating the total energy [Eq. (1)], the coupling of the self-energy and pair interactions to the Madelung potential provides effective many-body interactions, hence in general $C_{12} \neq C_{44}$. In fact, the sign of Δ $(=C_{12}-C_{44})$ is correctly predicted in all four cubic alkaline-earth oxides, a result not possible in breathing-shell models,[2,34] unless nonspherical deformations are allowed.[39] The results of the MEG calculation for MgO and CaO, in which a fixed Watson sphere was used, are also shown in Table III. The present calculation, in which the Watson sphere is allowed to expand and compress with deformation of the crystal, gives generally better agreement with experiment for the individual moduli.

IV. PRESSURE-VOLUME RELATIONS

Within the parametrized version of PIB outlined in Sec. II it is straightforward to calculate the equation of state.

TABLE III. Second-order elastic moduli.

	K[a]		C_{11}		C_{12}		C_{44}		C_s[b]		Δ[c]	
	Calc.	Expt.[d]	Calc.	Expt.[d]	Calc.	Expt.[d]	Calc.	Expt.[d]	Calc.	Expt.[d]	Calc.	Expt.[d]
MgO	1.39	1.63[e]	2.70	2.97[e]	0.73	0.95[e]	1.27	1.56[e]	0.99	1.01[e]	−0.54	−0.61[e]
	1.70[f]		2.26[f]		1.42[f]		1.42[f]		0.42[f]		0.00[f]	
CaO	1.02	1.14	2.06	2.23	0.50	0.59	0.66	0.81	0.78	0.82	−0.16	−0.22
	1.34[f]		2.07[f]		0.97[f]		0.97[f]		0.55[f]		0.00[f]	
SrO	0.80	0.89	1.71	1.74	0.34	0.47	0.49	0.56	0.69	0.64	−0.15	−0.09
BaO	0.66	0.74	1.33	1.74	0.33	0.49	0.31	0.34	0.50	0.38	+0.02	+0.15

[a]Bulk modulus, $K=\frac{1}{3}(C_{11}+C_{12})$.
[b]Shear modulus, $C_s=\frac{1}{2}(C_{11}-C_{12})$.
[c]Cauchy violation, $\Delta=C_{12}-C_{44}$.
[d]Experimental data from Chang and Graham (Ref. 12), except where noted.
[e]Experimental data from Jackson and Niesler (Ref. 13).
[f]MEG, Cohen and Gordon (Ref. 3).

TABLE IV. Pressure derivatives of the elastic moduli at zero pressure.

	K'[a]		C_s'[b]		C_{44}'		Δ'[c]	
	Calc.	Expt.[d]	Calc.	Expt.[d]	Calc.	Expt.[d]	Calc.	Expt.[d]
MgO	4.18	4.13[e]	3.60	3.78[e]	0.79	1.11[e]	1.00	0.50[e]
	4.02[f]		2.42[f]		0.41[f]		2.00[f]	
CaO	4.33	4.85	3.88	4.14	0.07	0.20	1.67	1.89
	4.09[f]		2.85[f]		0.19[f]		2.00[f]	
SrO	4.44	5.23	4.12	4.34	0.04	−0.21	1.66	2.55
BaO	4.55	5.67	3.84	3.49	−0.30	−0.47	2.29	3.81

[a]$K'=\frac{1}{3}(C_{11}'+2C_{12}')$.
[b]$C_s'=\frac{1}{2}(C_{11}'-C_{12}')$.
[c]$\Delta'=C_{12}'-C_{44}'$.
[d]Experimental data from Chang and Graham (Ref. 12), except where noted.
[e]Experimental data for MgO from Jackson and Niesler (Ref. 13).
[f]MEG, Cohen and Gordon (Ref. 3).

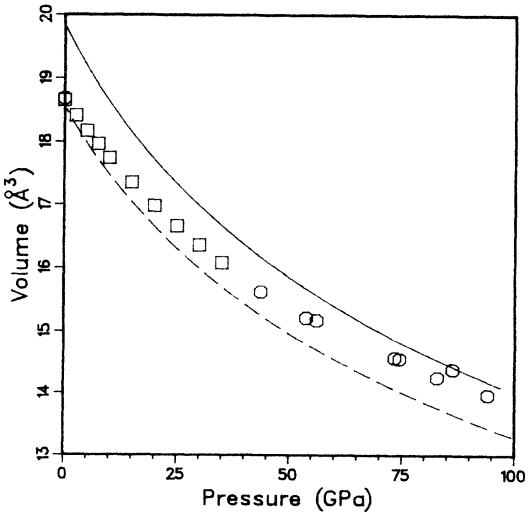

FIG. 2. Calculated PIB equation of state for the $B1$ and $B2$ phases of MgO and experimental data from Ref. 14 (squares) and Ref. 15 (circles).

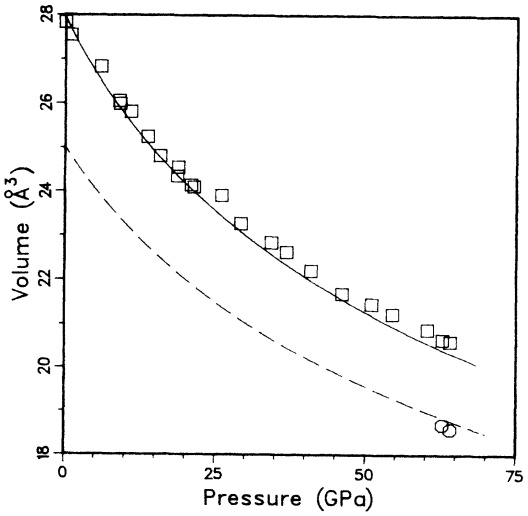

FIG. 3. Calculated and experimental equation of state for the $B1$ and $B2$ phases of CaO. The experimental data are from Ref. 16.

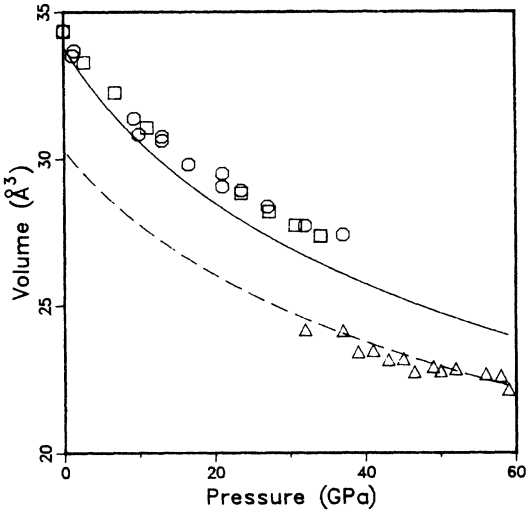

FIG. 4. Calculated and experimental equation of state for the $B1$ and $B2$ phases of SrO. The experimental data are from Ref. 18 (squares) and Ref. 19 (circles and triangles).

The pressure as a function of volume is calculated from $P(V)=-d\Phi(V)/dV$ and $P(V)$ is inverted to provide the usual equations of state. The second derivative of the energy with respect to volume gives the bulk modulus, viz., $K=-V(d^2\Phi/dV^2)$, which can be written as a function of pressure or volume.

Experimental volume versus pressure data are available for the $B1$ phases of the alkaline-earth oxides considered here and for the $B2$ phases of CaO and SrO.[14–20] The P-V equations of state calculated from the PIB model for the $B1$ and $B2$ phases of the four compounds are compared with the available experimental data in Figs. 2–5. In all cases PIB is within 5% of the experimental data. Note that the agreement with the experiment is particularly good for the low- and high-pressure phases of CaO and for the high-pressure phase of SrO. For BaO, the calculated $B2$ compression curve is shown; according to experiment this compound appears to transform to a distorted $B2$ structure.

V. PRESSURE AND VOLUME DEPENDENCE OF THE C_{ij}

In this section we use the PIB model to study the behavior of the elastic moduli under pressure. The method is that used in Sec. III: at a fixed volume, the equilibrium pressure and elastic moduli are found by making small distortions to the cubic lattice and calculating the corresponding derivatives. Experimentally, the pressure derivatives of the elastic moduli at zero pressure have been determined.[9–13] The results of the PIB calculation are compared to experiment in Table IV. The theoretical model correctly predicts the observed trends as M goes from Mg to Ba. The results of the MEG calculation[3] are also shown for MgO and CaO. Again the PIB model gives generally better agreement with experiment than does the rigid-ion theory. According to the high-pressure Cauchy condition, $\Delta(P)=C_{12}-C_{44}=2P$, i.e., $\Delta'=2$ (see Ref. 3). The deviation from this relation provides another measure of the many-body interactions in the crystal. Values for Δ' that are both larger and smaller than 2 are calculated from the model. This is observed experimentally as well, although the measured range of values is larger than that calculated.

The elastic moduli have also been calculated explicitly at high pressure in the $B1$ and $B2$ phases of the oxides. The pressure dependence of C_{11}, C_{12}, and C_{44} are shown for MgO in Figs. 6 and 7. Also included is the pressure dependence of the quantity $C_{12}-C_{44}-2P$. From Fig. 6 one can see that the deviation increases with increasing pressure for MgO. Similar results are found for the other oxides, although for BaO $C_{12}-C_{44}-2P$ increases with pressure. For each compound the shear modulus C_{44} is found to decrease monotonically at high compression in the $B1$ phase. On the other hand, C_{44} increases with

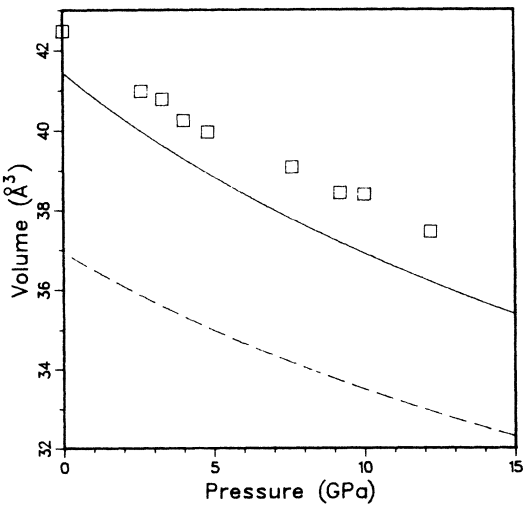

FIG. 5. Calculated equation of state for the $B1$ and $B2$ phases of BaO and experimental data for the $B1$ phase (Ref. 20).

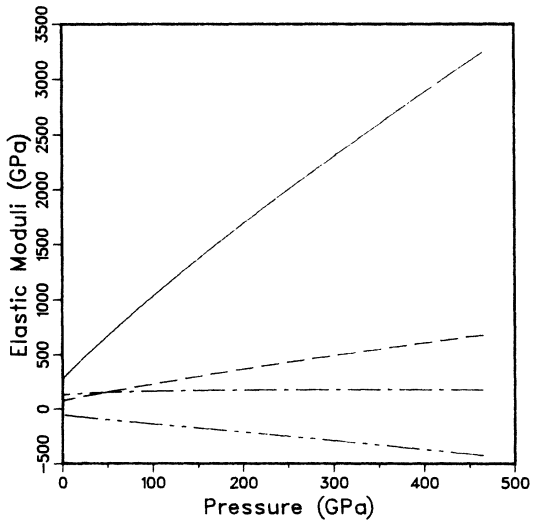

FIG. 6. Pressure dependence of the elastic moduli of MgO ($B1$). C_{11} (solid line), C_{12} (dashed line), C_{44} (dashed-dotted line), and $C_{12}-C_{44}-2P$ (dashed-double-dotted line).

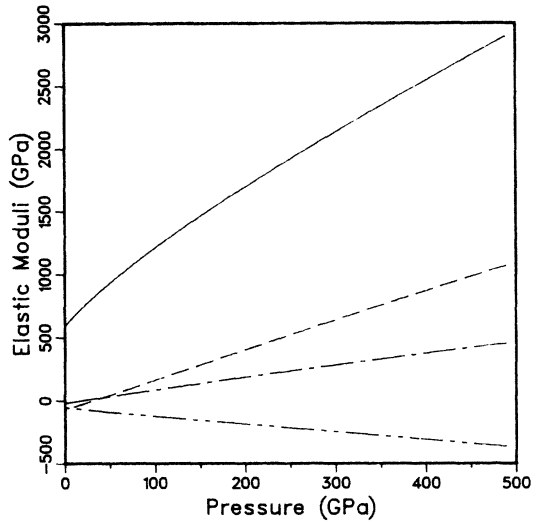

FIG. 7. Pressure dependence of the elastic moduli of MgO ($B2$). C_{11} (solid line), C_{12} (dashed line), C_{44} (dashed-dotted line), and $C_{12}-C_{44}-2P$ (dashed—double-dotted line).

pressure in the $B2$ phase. With the exception of BaO, C_{12} is found to be negative at $P=0$ for the $B2$ phases of all of the compounds. In addition, C_{44} is negative for MgO at $P=0$ in this structure. In other words, the $B2$ phase of this compound is elastically unstable with respect to a shear distortion at low pressure and is therefore predicted to be nonquenchable from high pressure.

Examining the volume dependence of elastic moduli is important for studying thermal expansion. The behavior of the elastic moduli as a function of volume for MgO ($B1$) is shown in Fig. 8. The shear modulus C_s vanishes at a volume of about 27 Å^3, corresponding to a lattice constant of 4.76 Å. Beyond this volume the lattice is unstable with respect to a distortion in which the lattice stretches along one of the three cubic axes and contracts

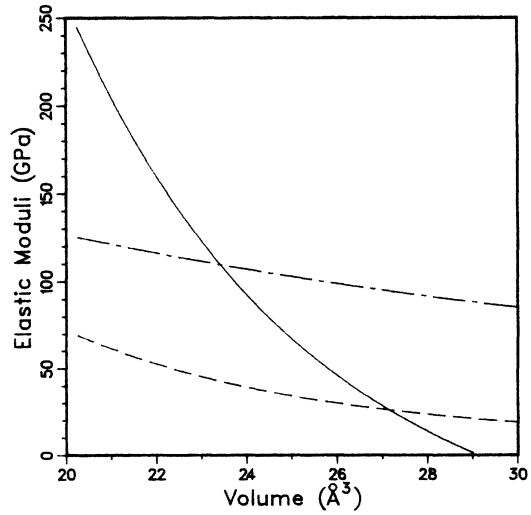

FIG. 8. Volume dependence of the elastic moduli of MgO ($B1$). C_{11} (solid line), C_{12} (dashed line), and C_{44} (dashed-dotted line).

in the plane perpendicular to the stretch. In alkali halides it has been shown that this type of instability is related to the melting transition.[40,41] The pressure dependence of the bulk modulus is also important in calculating the melting curve of an ionic solid.[41]

VI. PHASE TRANSITIONS

In the preceding discussions it was assumed that the $B1$ (rocksalt) phase was the ground state for these oxide crystals. Experimentally, this is true, but the Gordon-Kim—type models occasionally have difficulty predicting the proper ground state. For example, with free-ion charge densities the Gordon-Kim model predicts that lithium fluoride is stable in the zinc-blende ($B3$)-type structure.[4] To test that the $B1$ phase is indeed the equilibrium phase of the alkaline-earth oxides within PIB, the energy per molecule was calculated as a function of volume per molecule for six lattices. The first three have cubic space groups: (1) $B1$ (rocksalt); (2) $B2$ (cesium chloride); (3) $B3$ (zinc-blende). The other three are hexagonal: (4) the tungsten carbide structure; and two nickel arsenide structures, with (5) the oxygen ion (O); and (6) the metal ion (M) on the arsenic site.[42] The hexagonal lattices are allowed to completely relax by adjusting the c/a ratio to minimize the total energy at each volume. The possibility that the first three phases will undergo a shear transition into a tetragonal phase with $c/a \neq 1$ is also considered.

The PIB results for MgO are shown in Fig. 9. The c/a ratio as a function of volume and the total energy per molecule are shown in Figs. 9(a) and 9(b), respectively. The cubic $B1$ phase, with no tetragonal distortion, is the predicted equilibrium phase of MgO. The PIB model finds that the $B1$ phase is the equilibrium phase for all of the alkaline-earth oxides, in agreement with experiment.

The model may also be used to study pressure-induced phase transitions. The transition occurs at the pressure P in which the Gibbs free energies of the two phases are equal. At absolute zero $G=\Phi+PV$, so it is easy to calculate the free energy as a function of pressure with the parametrized form of the energy. Table V lists the PIB transition pressures (P_{tr}) and volumes (V_{tr}).

The model predicts that a $B1$-$B2$ phase transition will occur under pressure in all of the MO compounds. The $B1$-$B2$ transition has been observed experimentally in CaO (Ref. 21) and SrO (Ref. 19). The calculated P_{tr} are in good agreement with experiment for these crystals in comparison with the earlier MEG theory,[3,43] although the predicted transition volumes are low (as is the case for MEG). The $B1$-$B2$ transition has not been observed in BaO, which transforms from the $B1$ phase to a tetragonal structure at 9.0 GPa,[20] well below the predicted $B1$-$B2$ transition. The PIB total energy for this low-symmetry structure has not been calculated, so we cannot predict the transition pressure.

No solid-solid phase transition has yet been observed experimentally in MgO.[44] Theoretical predictions for the $B1$-$B2$ transition range from 117 (Ref. 22) to 1050 GPa (Ref. 24). The PIB prediction of 250 GPa is nearly identical to that predicted by the MEG method of Cohen and

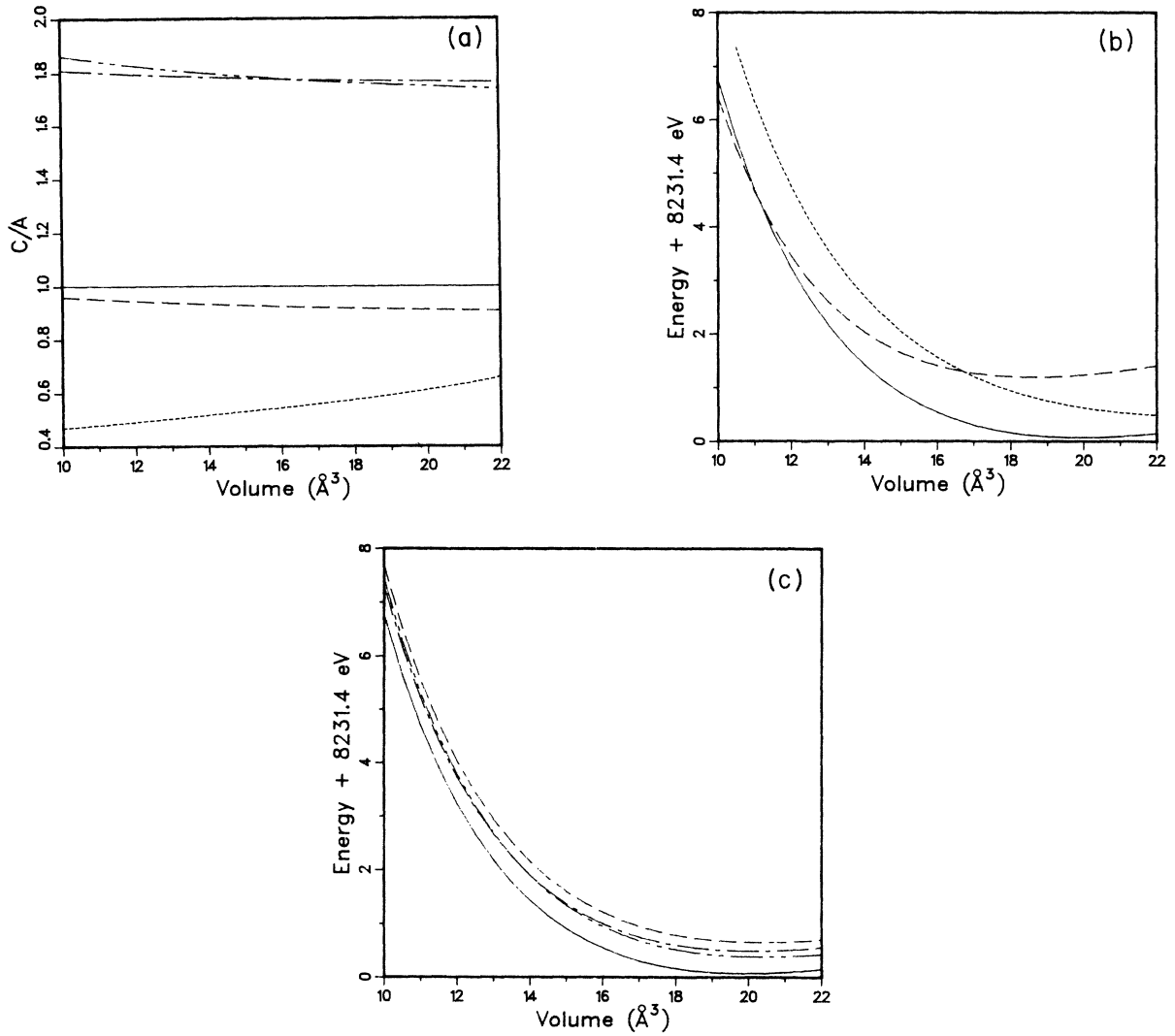

FIG. 9. Study of the possible equilibrium phases of MgO within the PIB model. (a) shows the c/a ratio which minimizes the energy per unit cell for a given structure at a given volume. The $B1$ and $B2$ phases (solid line) remain cubic at all pressures. Note that for the volumes shown here the zinc-blende ($B3$) (dotted line) structure undergoes a shear compression in the z direction. The notation for the hexagonal phases is as follows: tungsten carbide (dashed line); NiAs with O on the As site (dashed-dotted line); NiAs with Mg on the As site (dashed—double-dotted line. (b) and (c) show the total energy per unit cell versus volume for each phase, calculated at the c/a ratio given in part (a). (b) shows the $B1$ (solid line), $B2$ (dashed line), and $B3$ (dotted-line) phases, while (c) shows $B1$ (solid line), tungsten carbide (dashed line), and NiAs with O (dashed-dotted line), and Mg on the As site (dashed—double-dotted line).

Gordon[3] (but over a factor of 2 lower than the extended SSMEG model described in Ref. 7, where SSMEG is the shell-stabilized MEG). On the basis of thermochemical systematics, Navrotsky and Davies[45] have suggested that the high-pressure phase of MgO is not $B2$, but nickel arsenide. As seen in Fig. 9(b), there is no evidence that the NiAs structure is stable at any pressure according to the PIB model.

VII. DISCUSSION

A parameter-free model for the cubic alkaline earth oxides has been presented and shown to give a good account of both zero-pressure equilibrium properties and high-pressure behavior of these compounds. The most significant result of these calculations concerns the predicted zero-pressure elastic moduli for these oxide crystals. The calculated trends in the elastic moduli are found to be in good agreement with experiment. In particular, the Cauchy equality is broken for these crystals and the sign of Cauchy violation is correctly reproduced in each. In addition, the magnitude of the calculated moduli for MgO and CaO are generally in better agreement with experiment than are previous rigid-ion calculations (i.e., with fixed Watson spheres).

On the other hand, the zero-pressure elastic moduli for all crystals (except C_{11} for BaO) are too low, and the magnitude of the Cauchy violation is underestimated. The latter effect will be modified by including the thermal contribution in the theory. This contribution to the Cau-

TABLE V. $B1$-$B2$ transition.

	P_{tr}, GPa		$V_{tr}(B1)$, Å^3		$V_{tr}(B2)$, Å^3		$\Delta V_{tr}/V(B1)$, %	
	Calc.	Expt.	Calc.	Expt.	Calc.	Expt.	Calc.	Expt.
MgO	251 256[b]	>100[a]	11.3		10.8		−4.3	
CaO	55 121[b]	63[c]	20.9	20.7[c]	19.3	18.7[c]	−7.9	−10.0[c]
SrO	36 90[e]	36[d]	26.3	27.5[d]	24.2	24.1[d]	−7.9	−13.0[d]
BaO	21	9[f]	34.0		31.2		−8.3	

[a]Mao and Bell (Ref. 15).
[b]MEG model, Cohen and Gordon (Ref. 3).
[c]Mammone *et al.* (Ref. 16); see also Jeanloz *et al.* (Ref. 21).
[d]Sato and Jeanloz (Ref. 19).
[e]SSMEG, Hemley (Ref. 47).
[f]Tetragonal structure, Liu and Bassett (Ref. 20).

chy violation has been studied from the standpoint of rigid-ion theory for MgO and the alkali halides.[6,43,44] It is also likely that more accurate quantitative predictions for the elastic moduli for these oxide crystals will require further study of the density functionals that are used as well as different treatment of the charge density. Some evidence for this is seen by the ability of the model to predict other quantities. Although the present treatment is quite reasonable in predicting the equilibrium lattice constants of the four alkaline-earth oxides, previous calculations of the Gordon-Kim–type that use different approximations find somewhat better agreement, at least for MgO (Table I). It is therefore likely that further refinements in the theory will improve the quality of the results for the elasticity of these crystals. This point is elaborated further below.

As discussed above, the calculation of the pressure dependence of the elastic moduli of the simple oxides is relevant to solid-earth geophysics. It is common to expressed the pressure dependence of the elastic moduli in terms of the zero-pressure derivatives. Reliable predictions for these derivatives are important in geophysics. The improvement in the calculations of these quantities in comparison to the previous rigid-ion MEG calculations has been noted above. The best agreement between the present theory and experiment is obtained for MgO. Indeed, the calculated value of the pressure derivative of the bulk modulus K' is within the experimental error quoted by Jackson and Niesler for MgO.[13] At high pressure, however, the present theory overestimates the compressibility of MgO as shown in Fig. 2. This suggests the need to examine higher-order zero-pressure derivatives to model accurately the equation of state at high pressures.

The experimental trend in the pressure dependence of the shear moduli (C_s and C_{44}) for the four crystals is reproduced by the theory; that is, C_s' increases in going from MgO to SrO and then decreases for BaO, whereas C_{44}' decreases from MgO to BaO. Previous studies of the mechanism of the $B1$-$B2$ transition in rocksalt-type crystals have suggested a correlation between the softening of the C_{44} mode and the phase-transition pressure.[43,46,47] The drop in C_{44}' from MgO to SrO is consistent with this interpretation. As in the case of the alkali halides,[43] the high-pressure instability where C_{44} vanishes occurs well above the predicted $B1$-$B2$ phase-transition pressure.

The predicted transition pressures (P_{tr}) for the $B1$-$B2$ phase transition in CaO and SrO are very close to experiment. The extremely accurate result for SrO is probably fortuitous. The situation for CaO may be similar. Recent attempts at reversing the transition (i.e., decreasing the pressure from the $B2$ to the $B1$ stability field) suggest that the true thermodynamic boundary may in fact be closer to that calculated here.[17] It should be noted that whereas these systems have been studied at room temperature and the calculated P_{tr} apply to the static lattice, the $B1$-$B2$ phase boundaries for these oxides are estimated to be only weakly temperature dependent in this range.[48]

Despite the excellent agreement for P_{tr} for CaO and SrO, the theory underestimates the transition volumes (ΔV_{tr}). This discrepancy suggests that there may be a fortuitous cancellation of errors in the relative contribution of the internal energy Φ and the $P\Delta V$ terms in the Gibbs free energies of the $B1$ and $B2$ phases in the region of the phase transition. That Gordon-Kim–type calculations tend to underestimate ΔV_{tr} for CaO and SrO has been noted previously.[19] An earlier MEG calculation for SrO was in fairly good agreement with experiment for compressing of the $B1$ phase (see Refs. 19 and 48); however, the density of the $B2$ phase was significantly underestimated (i.e., ΔVt_{tr} at the experimental P_{tr} was smaller than experiment). In the present model the density of the $B2$ phase of SrO is in good agreement with experiment, but the compressibility of the $B1$ phase is too large. The self-consistent augmented-plane-wave calculations performed for MgO and CaO by Bukowinski[25] predict a larger volume difference between the $B1$ and $B2$ phases of these compounds than does the present model, particularly at very high pressure (> 100 GPa).

Gordon-Kim–type calculations have been most successful for low-Z elements (with the exception of H). It is therefore interesting that for BaO, the sign of the Cauchy

violation is correctly calculated (in contrast to the results of spherical shell models) and the calculated compressibility in the $B1$ phase is in good agreement with experiment. On the whole, however, the results for BaO are generally poorer than those for the other oxides studied (e.g., the magnitude of Δ and K'). It is likely that these problems are associated with quality of the wave function used for the Ba^{2+} ion. For a high-Z ion such as a Ba^{2+} electron-correlation effects may be quite significant. Furthermore, the low symmetry of the high-pressure phases of BaO suggests that nonspherical deformations of the charge density may be important in this crystal. The latter problem may require charge densities obtained from band-structure calculations,[49] as discussed below.

Finally, possible improvements in the fundamental theory employed here are discussed. In this study, the Thomas-Fermi expression has been used for the kinetic energy in both the expression for the self-energy of the ions and the pair interaction energies.[36] Indeed, in the present theory, the pair interaction energies can only be found within the Thomas-Fermi approximation. The accuracy of the approximation is shown by the good agreement with experimental lattice constants shown above. This agreement suggests that although the Thomas-Fermi approximation errs in calculating the total energy of the system, it correctly predicts the change in energy due to a distortion of the lattice.

In finding the cohesive energy of an ionic solid, however, one does not compare the total energies of two similar lattices, since in one "lattice" the ions are infinitely far apart. The pair interactions are only a small part of the cohesive energy (about 3 eV in MgO and CaO), the rest being due to the change in self-energy of the ions. It seems reasonable to use a better approximation for the kinetic-energy part of the ionic self-energy. Within the local-density approximation, the kinetic energy is exactly determined by the method of Kohn and Sham.[38] When this functional is used to calculate the self-energies of the ions, while still employing the Thomas-Fermi formalism for the pair energies, the cohesive energies listed in the third column of Table II are found. These calculations are in good agreement with experiment and with the calculations of Ref. 3, which are listed in the fourth column of Table II.

On the other hand, when the total energy is calculated as a function of volume with the Kohn-Sham self-energy, the predicted equilibrium lattice constants are 4.02 Å for MgO and 4.49 Å for CaO, significantly smaller than those found experimentally, or with the Thomas-Fermi version of PIB. The error in this approximation probably comes from the use of different energy functionals (Kohn-Sham and Thomas-Fermi) in the self-energy and the pair energy. To illustrate this point consider what happens when the lattice contracts: The PIB effect reduces the amount of overlap (from what it would be if ions were rigid) by moving charge from the tail region of the O^{2-} ion to a region nearer the oxygen ion nucleus. If two different functionals are used for the self-energy and pair potentials, part of the net charge by energy comes from this difference, which is unphysical. Recent work by Harris[50] suggests that one can improve upon the Thomas-Fermi pair energy while maintaining the spirit of the Gordon-Kim approximation. Studies in this area are in progress.

Another approach to improve the cohesive energies may be by the use of better charge densities within a PIB treatment. It should be pointed out that the Watson-sphere induced charge densities do not minimize the PIB crystal energy [Eq. (1)]. Better results may be obtained if variational parameters β_k are introduced to give in Eq. (1).

$$\Phi=\tfrac{1}{2}\sum_{k,l} Z_k P[{}^{l}_{k}]+\sum_{k,l} S_k\{\beta_k P({}^{l}_{k})\} + \tfrac{1}{2}\sum_{k,k',ll'} \phi[\beta_k P({}^{l}_{k}),\beta_{k'} P({}^{l'}_{k'}),\,|\,\mathbf{r}[{}^{l}_{k}]-\mathbf{r}[{}^{l'}_{k'}]\,|\,] \tag{5}$$

and with β_k chosen to minimize the energy for a given structure. As pointed out by Harris,[50] (1) is not the exact Hamiltonian of the system, so a variational minimization need not improve the agreement with experiment. Use of Eq. (5) will, however, increase the calculated cohesive energy, since Φ in (5) is necessarily less than or equal to Φ in (1).

Another possible improvement of PIB would be to use more accurate charge densities. As mentioned above, previous Gordon-Kim calculations for oxides have used spherical charge densities determined from Hartree-Fock theory.[3,-5,7] Another approach is to include nonspherical deformations of charge density. This extension could be accomplished by generating densities from APW calculations, as was done by Boyer,[6] but instead of using a rigid-ion model, charge densities could be calculated at different volumes.

ACKNOWLEDGMENTS

We would like to thank J. L. Feldman, R. E. Cohen, C. Y. Fong, J. R. Hardy, J. W. Flocken, and R. G. Gordon for useful discussions, and R. M. Hazen for review of the manuscript. Work carried out at the U. S. Naval Research Laboratory was supported by the U. S. Office of Naval Research (Materials Science Division).

APPENDIX: PAIR POTENTIALS AND PARAMETRIZATION

The pair potentials are calculated in a manner that is slightly different than found in the original Gordon and Kim paper.[23] First, the kinetic energy and exchange functionals (denoted as V_K and V_x, respectively), are identical to Gordon and Kim's, but for the correlation potential (denoted as V_c) the Hedin-Lundqvist parametrization is used.[30] The latter is the functional used to calculate the electron density in the Liberman program.[21] Second, the electrostatic interaction is divided into four parts, as follows. The charge density for the ith ion is written as

$$P_i(\mathbf{r})=Z_i\delta(\mathbf{r})-n_i(\mathbf{r})\,, \tag{A1}$$

where Z_i is the atomic number, $\delta(\mathbf{r})$ is the Dirac δ function, and $n_i(\mathbf{r})$ is the electron number density. Defining $N_i=\int d^3r\, n_i(\mathbf{r})$ as the number of electrons in the ith ion, the electrostatic interaction energy between ion i and ion j, separated by a vector $\mathbf{R}$ is

$$V_{eij}(R)=\frac{(Z_i-N_i)(Z_j-N_j)}{R}+Z_iP_{sj}(R)$$
$$+Z_jP_{si}(R)+V_{sij}(R)\ , \tag{A2}$$

where P_{si} is the short-range part of the electrostatic potential of the ith ion:

$$P_{si}(\mathbf{R})=\int d^3r\, n_i(\mathbf{r})\left[\frac{1}{|\mathbf{R}-\mathbf{r}|}-\frac{1}{R}\right] \tag{A3}$$

and $V_{sij}(\mathbf{R})$ is the short-range part of the interaction between the two electron distributions:

$$V_{sij}=\int d^3r\int d^3r'\, n_i(\mathbf{r})n_j(\mathbf{r}')\left[\frac{1}{|\mathbf{r}-\mathbf{r}'-\mathbf{R}|}-\frac{1}{R}\right]. \tag{A4}$$

The advantage of this form of the Coulomb interaction is that $P_{si}(\mathbf{R})>0$ and $V_{sij}(\mathbf{R})<0$ for all R, and both functions decay exponentially with increasing R. Evaluating the potentials in this fashion substantially reduces the roundoff error in the calculation.

As defined here, the electrostatic potentials P_s and the pair potentials $-V_s$, V_k, $-V_x$, and $-V_c$ are positive definite. They also decay exponentially at large R for exponentially decaying electron densities, allowing us to use a relatively simple form to parametrize the pair potentials. In doing this, one must account for the change in the potentials as a function of both the distance and the Madelung potentials at the ion sites. We fit the short-range electrostatic potentials to the form

$$P_{si}(P,R)=\exp[f_0^{(i)}(P)+f_1^{(i)}(P)(R-\bar{R})$$
$$+f_2^{(i)}(P)(R^{-1}-\bar{R}^{-1})]\ , \tag{A5}$$

where

$$f_k^{(i)}(P)=C_{k0}^{(i)}+C_{k1}^{(i)}(P-P_i)+C_{k2}^{(i)}(P-P_i)^2\ .$$

The pair potentials are fitted to the form

$$V_{tij}(P_i,P_j;R)=\alpha_i\exp[g_0^{(tij)}(P_i,P_j)+g_1^{(tij)}(P_i,P_j)(R-\bar{R})$$
$$+g_2^{(tij)}(P_i,P_j)(R^{-1}-\bar{R}^{-1})]\ , \tag{A6}$$

where $\alpha_i=+1$ for the kinetic-energy interaction and -1 for everything else, and

$$g^{(tij)}(P_i,P_j)=d_{k0}^{(tij)}+d_{k1}^{(tij)}(P_i-\bar{P}_i)+d_{k2}^{(tij)}(P_j-\bar{P}_j)+d_{k3}^{(tij)}(P_i-\bar{P}_i)^2+d_{k4}^{(tij)}(P_i-\bar{P}_i)(P_j-\bar{P}_j)+d_{k5}^{(tij)}(P_j-\bar{P}_j)^2\ ,$$

where $\bar{P}_i$, $\bar{P}_j$, and $\bar{R}$ are fixed parameters, usually taken to be the value at the midpoint of the range over which the fits are made. The term linear in R accurately accounts for the exponential decay of the Gordon-Kim pair interaction at large distances, and the $1/R$ term is used to provide better agreement at small values of R. It is not the correct form of the interaction as $R\to 0$, but the present applications of the model are concerned only with the region $R>1$. The quadratic fit to the potential parameters is adequate for the range of potentials discussed here.

The parametrization procedure is as follows: the range of Watson sphere potentials P required for each ion are determined first, along with the range of distances R needed for each pair interaction. The charge densities required for each ion are then calculated at several (usually on the order of 10) values of P in the required range. The value for $P_{si}(R)$ at a suitable number of points for each P, and $V_{tij}(R)$ ($t=s$; k, x, or c) for each P_i and P_j, and a similar mesh of R values are then found. These values are then fitted to (A5) and (A6) by the method of linear least squares, fitting the logarithm of the potential to the logarithm of (A5) and (A6). Typically, the fit is within 5% of the true potential at any point within the range of the fit, with the largest errors being made at the endpoints. As shown in Sec. II, the fit is adequate so long as unit cell volumes are kept within reasonable bounds. The values for the parameters are available from the authors on request.

*Also at Sachs/Freeman Associates, Bowie, MD 20716.

[1]M. Born and K. Huang, *Dynamical Theory of Crystal Lattices*, (Clarendon, London, 1954).
[2]See, C. R. A. Catlow, M. Dixon, and W. C. Mackrodt, in *Computer Simulation of Solids*, edited by C. R. A. Catlow and W. C. Mackrodt (Springer-Verlag, New York, 1982), p.132.
[3]A. J. Cohen and R. G. Gordon, Phys. Rev. B **14**, 4593 (1976).
[4]C. Muhlhausen and R. G. Gordon, Phys. Rev. B **23**, 900 (1981).
[5]C. Muhlhausen and R. G. Gordon, Phys. Rev. B **24**, 2147 (1981).
[6]L. L. Boyer, Phys. Rev. B **27**, 1271 (1983).
[7]R. J. Hemley, M. D. Jackson, and R. G. Gordon, Geophys. Res. Lett. **12**, 247 (1985).
[8]L. L. Boyer, M. J. Mehl, J. L. Feldman, J. R. Hardy, J. W. Flocken, and C. Y. Fong, Phys. Rev. Lett. **54**, 1940 (1985).
[9]Z. P. Chang and G. R. Barsch, J. Geophys. Res. **74**, 3291 (1969); J. Phys. Chem. Solids **32**, 27 (1971).
[10]H. Spetzler, J. Geophs. Res. **75**, 2073 (1970).
[11]P. R. Son and R. A. Bartels, J. Phys. Chem. Solids **33**, 819 (1972); R. A. Bartels and V. H. Vetter, *ibid.* **33**, 1991 (1972).
[12]Z. P. Chang and E. K. Graham, J. Phys. Chem. Solids **38**, 1355 (1977).
[13]I. Jackson and H. Niesler, in *High-Pressure Research in Geophysics*, edited by S. Akimoto and M. H. Manghnani (Academic, Tokyo, 1982), p. 93.
[14]E. A. Perez-Albuerne and H. G. Drickamer, J. Chem. Phys. **43**, 1381 (1965).
[15]H. K. Mao and P. M. Bell, J. Geophys. Res. **84**, 4533 (1979).
[16]J. F. Mammone, H. K. Mao, and P. M. Bell, Geophys. Res. Lett. **8**, 140 (1981).
[17]P. Richet, H. K. Mao, and P. M. Bell (private communica-

tion).
[18]L. G. Liu and W. A. Bassett, J. Geophys. Res. **78**, 8470 (1973).
[19]Y. Sato and R. Jeanloz, J. Geophys. Res. **86**, 11773 (1981).
[20]L. G. Liu and W. A. Bassett, J. Geophs. Res. **77**, 4934 (1972).
[21]R. Jeanloz, T. J. Ahrens, H. K. Mao, and P. M. Bell, Science **206**, 829 (1979).
[22]K. J. Singh and S. D. Sanyal, Phys. Status Solidi B **113**, K23 (1983).
[23]Y. Yamashita and S. Asano, J. Phys. Soc. Jpn. **52**, 3506 (1983).
[24]K. J. Chang and M. L. Cohen, Phys. Rev. B **30**, 474 (1984).
[25]M. S. T. Bukowinski, Geophys. Res. Lett. **12**, 536 (1985).
[26]F. Birch, J. Geophys. Res. **57**, 227 (1952).
[27]R. Jeanloz and A. B. Thompson, J. Geophys. Res. **21**, 51 (1983).
[28]D. A. Liberman, D. T. Cromer, and J. J. Waber, Comput. Phys. Commun. **2**, 107 (1971).
[29]R. E. Watson, Phys. Rev. **111**, 1108 (1958).
[30]R. G. Gordon and Y. S. Kim, J. Chem. Phys. **56**, 3122 (1972).
[31]Y. S. Kim and R. G. Gordon, Phys. Rev. B **9**, 3548 (1974); A. J. Cohen and R. G. Gordon, *ibid.* **12**, 3228 (1975).
[32]J. P. Perdew and A. Zunger, Phys. Rev. B **23**, 5048 (1981). For simplicity, we use their averaged potential (75).
[33]L. Hedin and B. I. Lundqvist, J. Phys. C **4**, 2064 (1971).
[34]U. Shroeder, Solid State Commun. **4**, 347 (1966).
[35]P. P. Ewald, Ann. Phys. (Leipzig) **64**, 253 (1921).
[36]M. Abramowitz and I. A. Stegun, *"Handbook of Mathematical Functions"* (U.S. GPO, Washington, D.C., 1972), p. 883.
[37]*CRC Handbook of Chemistry and Physics, 61st ed.,* edited by R. C. Weast and M. J. Astle (Chemical Rubber Co., Boca Raton, Florida, 1981).
[38]W. Kohn and L. J. Sham, Phys. Rev. **140**, A1133 (1965).
[39]M. J. Sangster, J. Phys. Chem. Solids **35**, 195 (1974).
[40]M. Mehl and L. L. Boyer, Phys. Rev. Lett. **54**, 1404 (1985).
[41]L. L. Boyer, Phase Transitions **5**, 1 (1985).
[42]J. C. Slater, *Quantum Theory of Molecules and Solids* (McGraw-Hill, New York, 1965), Vol. 2, Chap. 3.
[43]R. J. Hemley and R. G. Gordon, J. Geophys. Res. **90**, 7803 (1985).
[44]L. L. Boyer, Phys. Rev. B **23**, 3673 (1981).
[45]A. Navrotsky and P. K. Davies, J. Geophys. Res. **86**, 3689 (1981).
[46]See, H. H. Demarest, Jr., R. Ota, and O. L. Anderson, in *High-Pressure Research: Applications in Geophysics,* edited by M. H. Manghnani and S. Akimoto (Academic, New York, 1977), pp. 281–301.
[47]S. Webb, Ph.D. thesis, Australian National University, 1985.
[48]R. J. Hemley (unpublished).
[49]M. S. T. Bukowinski and J. Hauser, Geophys. Res. Lett. **7**, 689 (1980).
[50]J. Harris, Phys. Rev. B **31**, 1770 (1985).